Supplementary Information

Mixed-ligand ZIF-doped perovskite films toward damp-heat stable solar cells

Shuaikang Chang,[#,a] Zuoming Jin,[#,a,b] Yu Wang,[#,a] Siyuan Lin,[a] Xueqian Han,[a]

Liqiang Zhang,[a] Yuanqiang Wang,[a] Jia Liang,[b] Yichuan Rui,[*,a]

[a]*College of Chemistry and Chemical Engineering, Shanghai University of*

Engineering Science, Shanghai 201620, P. R. China

[b]*College of Smart Materials and Future Energy, State Key Laboratory of Photovoltaic*

Science and Technology, Fudan University, 220 Handan Road, Shanghai 200433,

China

[#]*The authors contributed equally to this work.*

**E-mail: ryc713@126.com*

1. Experimental Section

1.1 Synthesis of ML-ZIF

The synthesis procedure of ML-ZIF is as follows: 2-MeIM (0.4 g/4.0 mmol) and 2-MIM (0.32 g/4.0 mmol) were dissolved in a mixed solvent of equal volumes ratio of DMF and EtOH (30 mL for each solvent) to obtain a solution A. $Zn(NO_3)_2 \cdot 6H_2O$ (0.595 g/2 mmol) was dissolved in an identical mixed solvent as above (30 mL each of DMF and EtOH) to obtain solution B. The solution A was then rapidly poured into the solution B and stirred for 2 h. Subsequently, the mixture was aged without disturbance for 24 h. The resulting ML-ZIF was collected by centrifugation at 8000 rpm, washed with EtOH and water, and finally re-dispersed in DMF for further use.

1.2 Preparation of Perovskite Solar Cells

First, an aqueous SnO_2 solution (15 wt%) was spin-coated onto FTO (3500 rpm, 30 s), followed by annealing at 150°C for 30 min to obtain the SnO_2 ETL. Subsequently, 250.4 mg PbI_2, 36.7 mg $PbBr_2$, 86.0 mg FAI, 11.2 mg MABr, and 25.8 mg CsI were dissolved in a mixed solvent of 400 mL DMF and 100 mL DMSO. The pre-dispersed ML-ZIF solutions of varying concentrations (0 mg/mL, 0.5 mg/mL, 1.0 mg/mL, and 1.5 mg/mL) were added to prepare MI-ZIF modified perovskite precursor solutions. These perovskite precursor solutions were spin-coated onto the SnO_2 substrate via a one-step method, which was spin-coated onto the SnO_2 surface at 4000 rpm for 30 s, with 200 μL chlorobenzene added during the last 10 s, followed by annealing at 105°C for 30 min (Fig. 2a). After natural cooling, Spiro-OMeTAD was spin-coated onto the perovskite film surface at 4000 rpm for 30 s. The Spiro-OMeTAD solution was prepared by dissolving 36.15 mg Spiro-OMeTA, 8.75 μL Li-salt, and 14.4 μL TBP in 550 μL chlorobenzene. After spin-coating, the samples were removed from the glovebox and placed in a dryer for Spiro-OMeTAD oxidation for 12 h. Finally, a 90 nm-thick gold layer was thermally evaporated onto the Spiro-OMeTAD surface to complete the device.

1.3 Characterization

X-ray diffraction (XRD) patterns were characterized using a Bruker D2 instrument with Cu Kα radiation, with 2θ scanning from 5° to 60°. Chemical bonds and functional

groups of the samples were analyzed using a Nicolet iS 10 Fourier transform infrared spectrometer. Film morphology was observed by field-emission scanning electron microscopy (FE-SEM, SU8010, Hitachi, Japan). Surface roughness was examined using a Bruker Dimension Icon atomic force microscope (AFM). UV-Vis spectrophotometry (Lambda 950, Perkin-Elmer Co.) was employed to characterize film transmittance and absorption spectra. X-ray photoelectron spectroscopy (XPS) was performed with Thermo Scientific ESCALAB 250Xi X-ray photoelectron spectrometer. Steady-state photoluminescence (PL) was measured using an FLS920 transient optical spectrometer (Edinburgh Instruments, UK). Current density-voltage (J-V) curves were recorded under AM 1.5 G illumination using a digital source meter (Keithley 2400), with light intensity calibrated to 100mW cm^{-2}. Electrochemical impedance spectroscopy (EIS) was performed in the dark using a Zahner-Elektrik workstation (Germany). Contact angles of different ETLs were characterized using an AST VCA Optima XE droplet shape analyzer. Film thermal conductivity was measured with a thermal conductivity instrument (TC3000E, Xiaxi Electronic Technology).

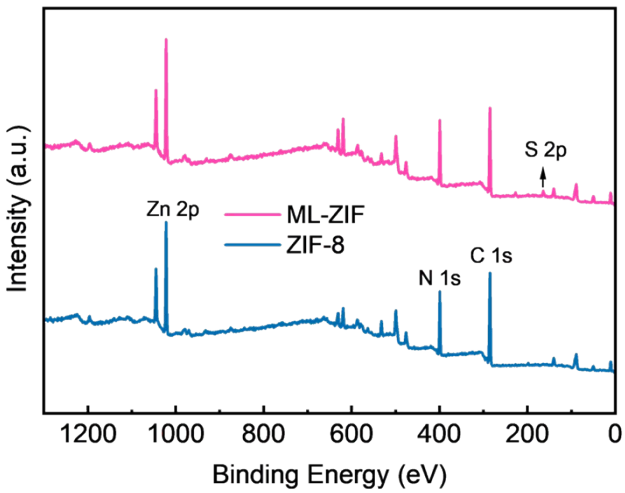

Fig. S1 XPS survey of ZIF-8 and ML-ZIF.

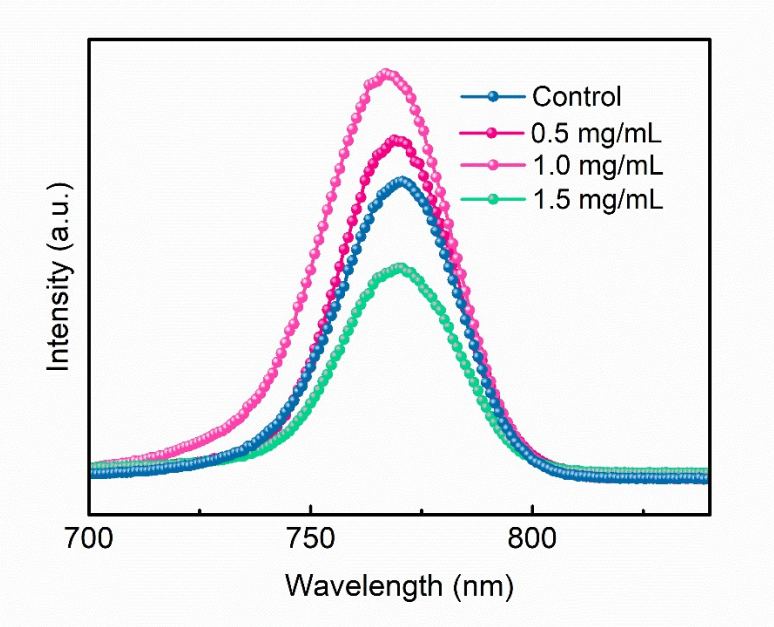

Fig. S2 Steady-state PL emission spectra of perovskite films with different doping concentrations.

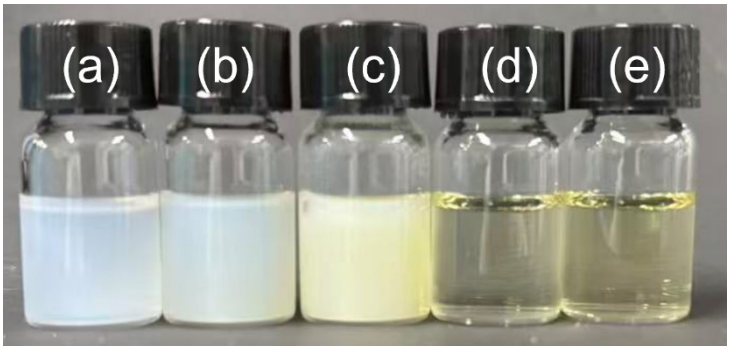

Fig. S3 Photographs of the products obtained from different 2-MeIM to 2-MIM molar ratios: (a) 0:4, (b) 1:3, (c) 1:1, (d) 3:1, and (e) 4:0.

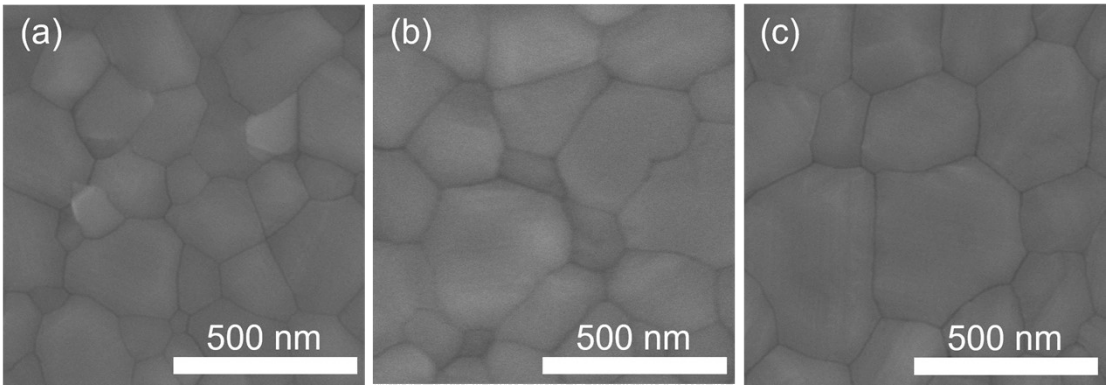

Fig. S4 SEM images of perovskite films doped with 1.0 mg/mL (a) ZIF-8 , (b) ML-ZIF (1:3) and (c) ML-ZIF (1:1).

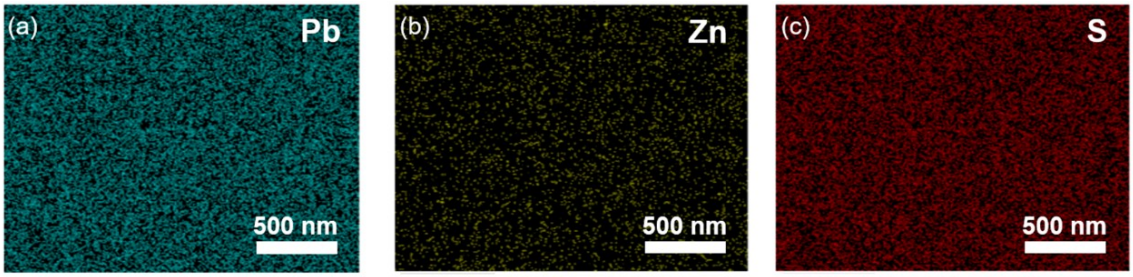

Fig. S5 EDS mappings of (a) Pb, (b) Zn, (c) S elements on the surface of ML-ZIF doped perovskite film.

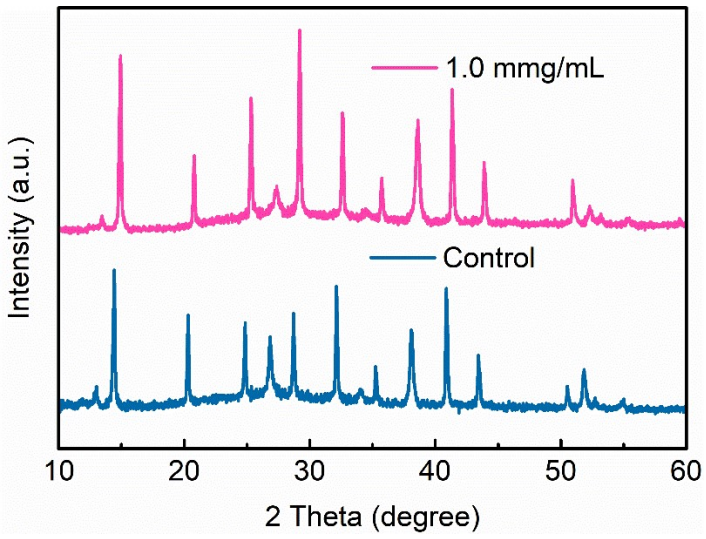

Fig. S6 XRD patterns of the control and ML-ZIF doped perovskite films.

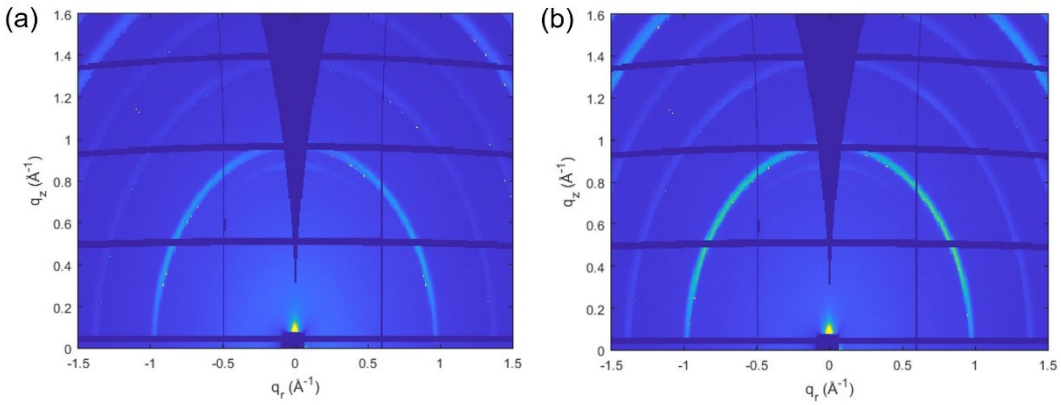

Fig. S7 GIWAXS images of (a) control and (b) ML-ZIF-doped perovskite films.

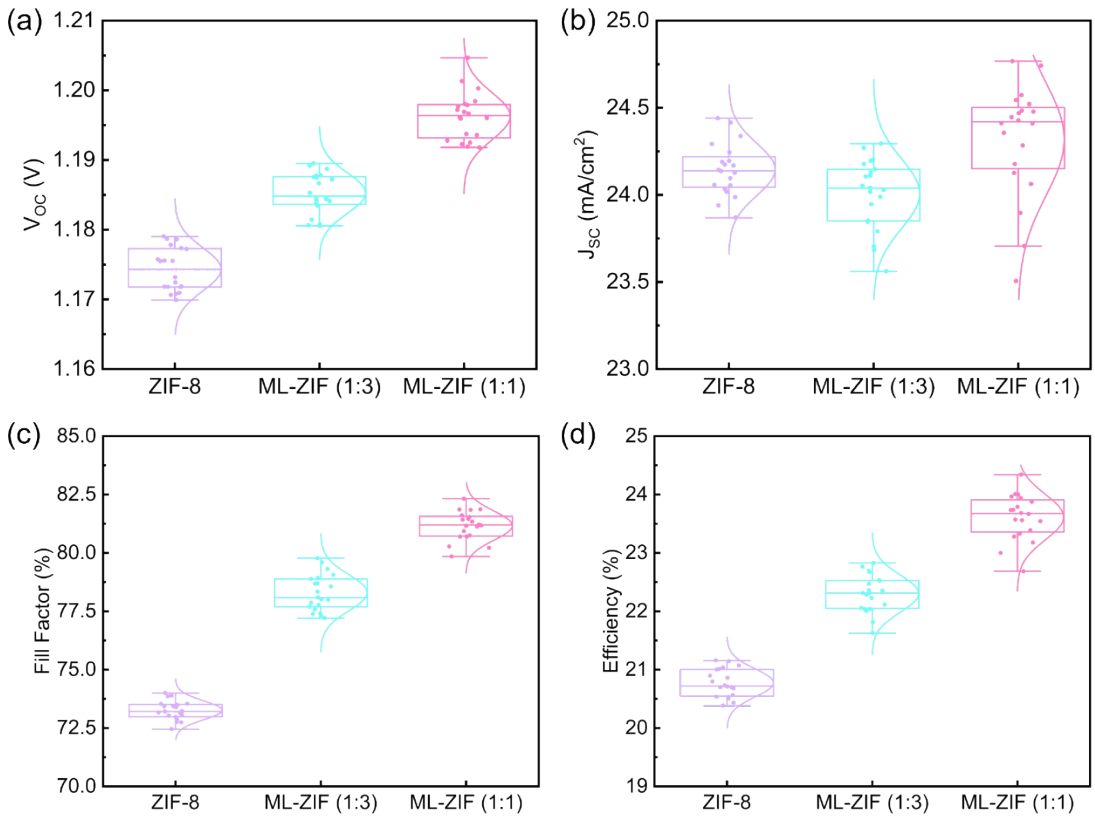

Fig. S8 The statistical data of PSC performance of V_{OC} (a), J_{SC} (b), FF (c), and PCE (d) for ZIF-8, ML-ZIF (1:3), and ML-ZIF (1:1).

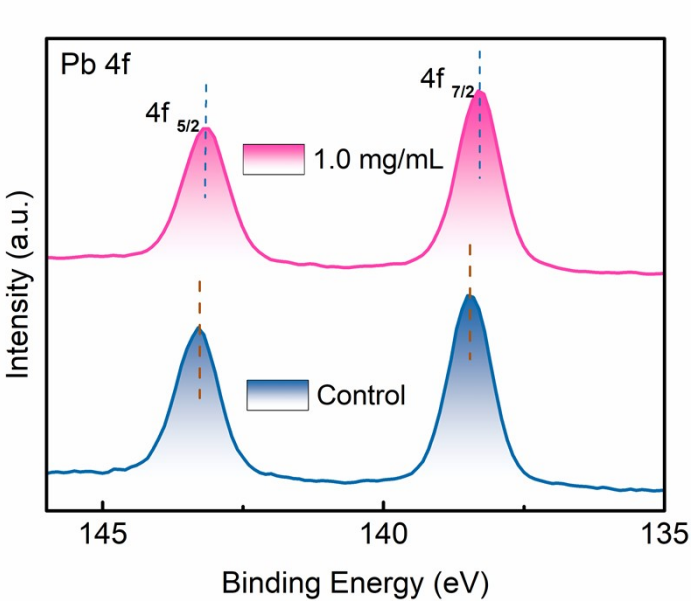

Fig. S9 Pb 4f XPS spectra of control and ML-ZIF-doped perovskite films.

Table S1 Photovoltaic parameters of the control and ML-ZIF-doped PSCs.

Samples		V_{oc} (V)	J_{sc} (mA cm^{-2})	FF (%)	PCE (%)
Control	Reverse	1.154	23.44	79.5	21.52
	Forward	1.130	23.26	78.6	20.66
ML-ZIF	Reverse	1.199	24.45	82.3	24.12
	Forward	1.196	24..48	81.1	23.74